

X-ray CT reveals 4D root system development and lateral root responses to nitrate in soil

Marcus Griffiths^{1,3}  | Nathan Mellor¹  | Craig J. Sturrock¹  |
 Brian S. Atkinson¹  | James Johnson² | Stefan Mairhofer² | Larry M. York^{1,4}  |
 Jonathan A. Atkinson¹  | Mohammadreza Soltaninejad²  | John F. Foulkes¹  |
 Michael P. Pound²  | Sacha J. Mooney¹  | Tony P. Pridmore²  |
 Malcolm J. Bennett¹  | Darren M. Wells¹ 

¹ School of Biosciences, Univ. of Nottingham, Sutton Bonington Campus, Loughborough LE12 5RD, UK

² School of Computer Science, Univ. of Nottingham, Jubilee Campus, Nottinghamshire NG8 1BB, UK

³ Donald Danforth Plant Science Center, St. Louis, MO 63132, USA

⁴ Biosciences Division, Oak Ridge National Laboratory, Oak Ridge, TN 37830, USA

Correspondence

Darren Wells, School of Biosciences, Univ. of Nottingham, Sutton Bonington Campus, Loughborough, LE12 5RD UK.

Email: darren.wells@nottingham.ac.uk

Assigned to Associate Editor Saoirse Tracy.

Funding information

European Research Council, Grant/Award Number: 294729; Biotechnology and Biological Sciences Research Council, Grant/Award Numbers: BB/L026848/1, BB/P016855/1, BB/P026834/1

Abstract

The spatial arrangement of the root system, termed *root system architecture*, is important for resource acquisition as it directly affects the soil zone explored. Methods for phenotyping roots are mostly destructive, which prevents analysis of roots over time as they grow. Here, we used X-ray microcomputed tomography (μ CT) to non-invasively characterize wheat (*Triticum aestivum* L.) seedling root development across time under high and low nitrate nutrition. Roots were imaged multiple times with the 3D models co-aligned and timestamped in the architectural plant model OpenSimRoot for subsequent root growth and nitrate uptake simulations. Through 4D imaging, we found that lateral root traits were highly responsive to nitrate limitation in soil with greater lateral root length under low N. The root growth model using all μ CT root scans was comparable to a parameterized model using only the final root scan in the series. In a second μ CT experiment, root growth and nitrate uptake simulations of candidate wheat genotypes found significant root growth and uptake differences between lines. A high nitrate uptake wheat line selected from field data had a greater lateral root count and length at seedling growth stage compared with a low uptake line.

1 | INTRODUCTION

The root system of a plant is a highly plastic organ for responding to the environmental availability of water and nutrients and nutritional status. Roots capture vital resources for the plant from the soil by intercepting passing water and solutes during rainfall events and foraging into new soil zones. A significant carbon investment and metabolic cost is associated

Abbreviations: DAS, days after sowing; HN, high nitrogen; LN, low nitrogen; NUp, Nitrate uptake; NUpE, Nitrogen-uptake efficiency; RSML, root system markup language; S×R DH, Savannah × Rialto winter wheat doubled haploid; μ CT, microcomputed tomography.

This is an open access article under the terms of the [Creative Commons Attribution](https://creativecommons.org/licenses/by/4.0/) License, which permits use, distribution and reproduction in any medium, provided the original work is properly cited.

© 2022 The Authors. *The Plant Phenome Journal* published by Wiley Periodicals LLC on behalf of American Society of Agronomy and Crop Science Society of America

with making and maintaining roots in a plant (Guo et al., 2021). Therefore, optimization in the four-dimensional (time and space) spatial arrangement of the root system is important and has the potential to greatly improve resource efficiencies (Morris et al., 2017; Rogers & Benfy, 2015). Improvement in resource capture by roots is needed to make more resilient cultivars that can maintain yield with lower fertilizer inputs.

Strategies to improve root system architecture are complex as the resources that plants need to forage differ in mobility and availability. Nitrate is highly soluble and mobile in the soil and can readily leach into deep soil layers and pollute groundwater. Root traits such as rooting depth that affect soil exploration have been shown to be important for resource capture and stress tolerance (Foulkes et al. et al., 2009; Ho et al., 2005; Lynch, 2013). In addition to where roots reside, variation in nutrient uptake rates occur among root classes, by root age, and plant nutrient status (reviewed in Griffiths & York, 2020). Understanding the effect of rooting and uptake traits on the rhizosphere will be important in directing breeding efforts and fertilizer management strategies.

A significant challenge in plant root phenotyping is the ability to nondestructively image and measure roots without disturbing the root system architecture or the soil environment in which the roots reside (Manske et al., 2001). Root phenotyping methods are often destructive involving root digging and washing, preventing analysis of roots over time. In vitro alternatives that allow root visualization during growth include agar, gel, and hydroponic-based systems (Atkinson et al., 2015; Nagel et al., 2020; Topp et al., 2013). However, root development of in vitro grown plants vary with that of soil due to differences in physical and chemical properties. In recent years, root-soil imaging techniques including X-ray microcomputed tomography (μ CT) and magnetic resonance imaging (MRI) are opening new opportunities in plant phenotyping for nondestructive rhizosphere imaging (Mooney, 2002; van Dusschoten et al., 2016). Using μ CT imaging, root and soil structure can be quantified at high resolution in 3D without disturbing the sample (Atkinson et al., 2020; Zhou et al., 2021). Analysis of such large volumetric image data is, however, a significant computational challenge with deep-machine learning approaches now being utilized to segment root material from soil, water, and air fractions (Soltaninejad et al., 2020).

Here we describe the use of μ CT imaging to characterize the root system architecture of wheat seedlings across time. Through 4D imaging, we revealed the development of the seminal and lateral root system and show that lateral root traits are highly responsive to nitrate application in soil. Comparing candidate genotypes selected from field data we found that a high nitrate uptake (NUp) line had greater lateral root count and length at seedling growth stage. These 4D μ CT scans were then used directly in a mathematical model of root NUp and

Core Ideas

- μ CT can non-invasively image root system development of plants across time.
- Wheat seedlings modify their root systems in response to N levels in soil.
- Simulation modeling can accurately predict root development and nitrate uptake.

soil nitrate depletion using the 3D root architectural model OpenSimRoot (Postma et al., 2017). The root growth and uptake model used could accurately predict seedling growth using only the final root shape as reference.

2 | MATERIALS AND METHODS

2.1 | Plant materials

Parents and selected members of the Savannah \times Rialto winter wheat doubled haploid (S \times R DH) mapping population were used in this study (Table S1). The S \times R DH population was supplied by Limagrain UK Limited. Lines were chosen based on contrasting nitrogen-uptake efficiency (NUpE; above-ground N uptake/N available (soil N + fertilizer N) performance from multi-year and site field trials (Atkinson et al., 2015). Seeds were sieved to a specific seed size range of 2.8–3.35 mm based on the mean of the parents to reduce any influence of variations in seed reserve size. The seeds were then laid out on germination paper (Anchor Paper Company) saturated with deionized water and stratified at 4°C in a controlled environment room for 5 d in darkness. After stratification, seeds were transferred to a controlled environment chamber at 20/15°C, 12-h, in darkness. After 48 h, the seeds had uniformly germinated with \sim 5 mm radicle length.

2.2 | Soil column preparation, μ CT root scanning and analysis pipeline for seedling studies

Soil mixtures were prepared using a <2 mm calibrated graduated sieve (Scientific Laboratory Supplies Ltd.) and compost mixer (Alvan Blanch Development Company Ltd.). The mixture was formulated to oven-dry soil weight dried at 105°C for 48 h (Rowell, 1994). Available N in the soil mixtures were determined by a United Kingdom Accreditation Services accredited commercial laboratory (NRM Laboratories, Bracknell, UK). PVC soil columns (75 mm [internal diameter] \times 170 mm [height]) were cut to size using a pipe

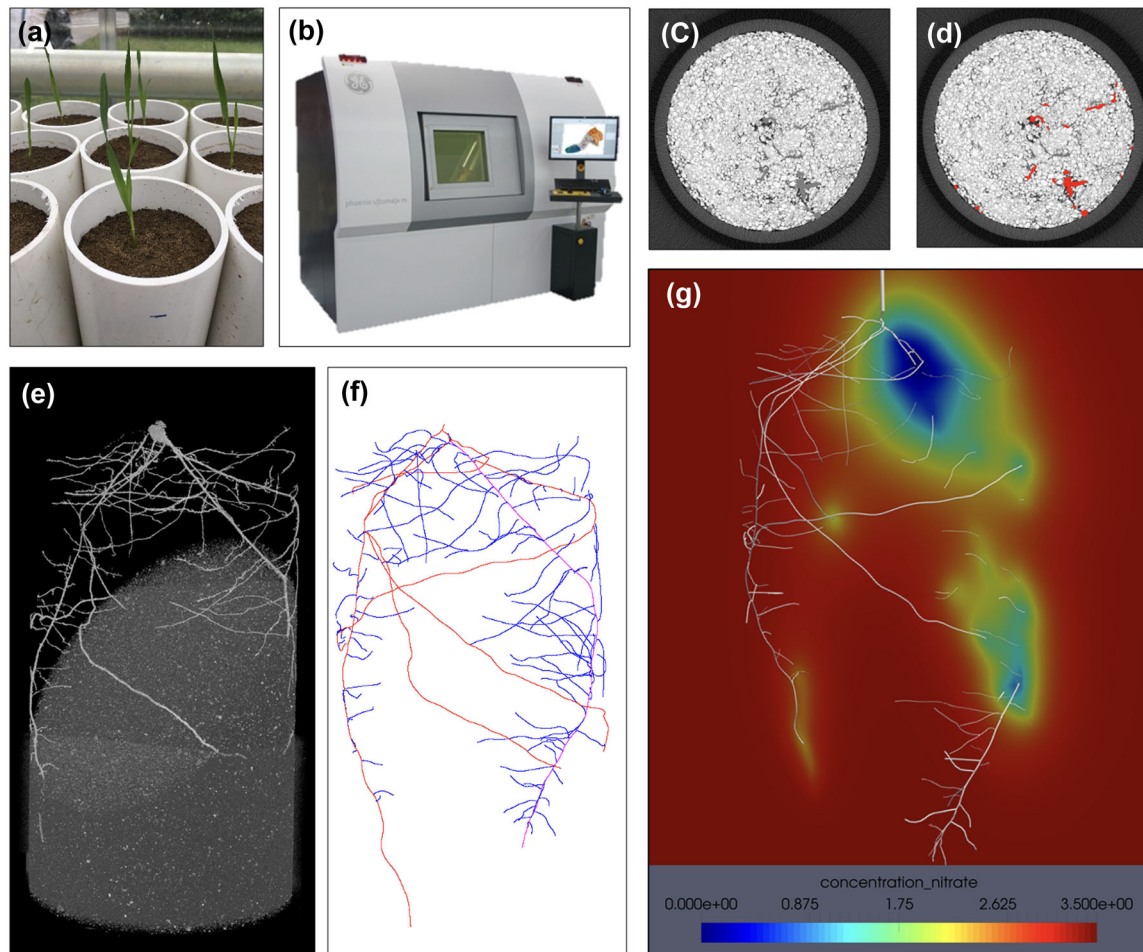


FIGURE 1 Microcomputed tomography (μ CT) 3D seedling root phenotyping pipeline. (a) Wheat seedlings growing in 75 mm [w] \times 170 mm [h] soil columns. (b) Phoenix vltomelx m $\text{\textcircled{R}}$ μ CT scanner. (c) Example μ CT z axis image slice of soil column. (d) μ CT image slice with segmented root material shown in red using RooTrak/VGStudio Max software. (e) Render of a wheat root system grown in soil that has been sliced to make roots visible. (f) Skeletonisation and extraction of quantitative root system architecture traits using RooTh software. Root classification is depicted with pseudo colors with primary seminal in purple, seminal roots in red, and lateral roots in blue. (g) OpenSimRoot model simulation using root system markup language (RSML) output from RooTh for a growing root system model with pseudo colors representing N depletion from 3.5 mM in red to zero in blue

cutter and a fine gauge curtain mesh was fastened to the bottom. The columns were evenly packed using air dried soil. The soil columns were then irrigated by capillary rise with the columns placed in a water tank for 24 h (Mairhofer et al., 2018). Saturated soil columns were allowed to dry for 48 h for determination of field capacity weights. With soil columns at field capacity, one pregerminated seedling was sown per column at approximately 15 mm soil depth (Figure 1a). Experiment specific details are detailed in Sections 3.3 and 3.4.

Soil columns were scanned using a Phoenix vltomelx m $\text{\textcircled{R}}$ industrial μ CT scanner (GE Measurement & Control Solutions) (Figure 1b). Prior to μ CT scanning, the soil columns were not watered for 2 d to ensure a high level of contrast between root and background. All columns were scanned with a 0.2-mm copper filter on the X-ray tube, at a potential energy of 160 Kv, current of 200 μ A, collecting 1,800 projection

images over a 360-degree rotation with a detector exposure timing of 250 ms, image averaging of 2, and a skip of 1. To image the entire 170-mm column height at a voxel resolution of 54 μ m, three individual scans were collected (top, middle, and bottom) and digitally stitched together following image reconstruction. The three scans for each column were completed in 69 min. The projection images of the scan were reconstructed into a 32-bit volume using Phoenix Datoslx REC software (GE Measurement & Control Solutions) with the application of a beam hardening correction value of 8. The top and bottom of the projections (approx. 200 pixels in Z axis for each) were excluded from the reconstruction to remove cone beam artifacts. The root system architecture was then extracted from the reconstructed soil volume using automatic root segmentation software RooTrak (Mairhofer et al., 2014) and VGStudio Max $\text{\textcircled{R}}$ v2.2.5 (Volume Graphics GmbH)

based on greyscale intensity values and root morphological features (Figure 1c–e). The root systems were subsequently used to train a deep machine learning approach for root segmentation (Soltaninejad et al., 2020). Data analysis in this study was performed using the original segmentations. Following root segmentation from the soil, the segmented root volume was skeletonized into a nested root system skeleton using RooTh (Mairhofer et al., 2018) (Figure 1f). RooTh was used to extract a root skeleton in the root system markup language (RSML) file format (Lobet et al., 2015) for each root scan and to measure root length and angle traits (Table S2). Global root traits that were not available in RooTh, such as convex hull, were calculated from the binary root image stack using RooTrak (Table S2) (Mairhofer et al., 2014). Root NUp simulations using the skeletonized root systems were then conducted using OpenSimRoot as described in Section 3.3 (Postma et al., 2017) (Table S2) (Figure 1g).

Destructive harvesting was conducted after the final μ CT scan of the time-series. The root system was severed from the shoot and washed from the soil material using a root washer (Hydropneumatic Elutriation System, Gillison's Variety Fabrication, Inc.) based on the work of Smucker et al. (1982). The roots were washed for 15 min and then immediately stored at -20°C for subsequent analysis. Roots were subsequently thawed, spread out on a clear waterproof tray, and then imaged on a flatbed scanner at 600 dpi resolution with a transparency unit (Epson Perfection v700; Regent Instruments Inc.). The 2D root scans were analyzed using WinRhizo® software v2002 (Regent Instruments Inc.) (Arsenault et al., 1995). After scanning, the roots and the shoots were dried at 80°C for 48 h for determination of dry biomass.

2.3 | Time-series of wheat root development in soil under varying N nutrition

A high NUpE wheat line from the S×R DH mapping population, identified in high nitrogen (HN) and low nitrogen (LN) field trials (Line 47) was used in a temporal seedling study under varying soil N nutrition (Table S4). A sandy-loam soil obtained from a long-term unfertilized field at Ryton Gardens Farm, Warwickshire, UK (52.37°N , 1.42°W) was prepared (1.3 g cm^{-3} bulk density). The soil mixture available total nitrogen (N) was determined as 5.22 mg kg^{-1} (nitrate 2.74 mg kg^{-1} , ammonium 2.48 mg kg^{-1}) (NRM Laboratories). Eight columns were prepared, half of which were irrigated with $10\text{ mM Ca}(\text{NO}_3)_2$ solution and the remaining irrigated with deionized water. The nitrate availability of the soil mixture represented a concentration typically found in unfertilized agricultural soils with the high nitrate treatment representative of the range found in fertilized soils and low affinity transport conditions (Lark et al., 2004; Miller et al., 2007; Zhu et al., 2021). Columns were placed in a glasshouse (four

replicates for each treatment, 27 March 2016–9 April 2016, temperature range $20/6^{\circ}\text{C}$, 12.5 h photoperiod). A plastic disk with a cut-out for the shoot was placed on top of the soil surface to reduce evaporation from the soil. No additional irrigation was provided during the growth period. Eight soil columns were μ CT scanned every 48 h from 0 to 12 DAS. At each μ CT imaging timepoint, a side-viewpoint image of the shoot was taken using a mounted digital SLR camera (Canon EOS 700D, Canon Inc.).

2.4 | Simulation modelling of μ CT scanned roots using OpenSimRoot

Nitrate uptake of wheat seedlings and soil nitrate depletion zones were simulated using the model framework OpenSimRoot (Postma et al., 2017). Basic nitrate and water modules were used as supplied in the OpenSimRoot repository, but root growth was prescribed so that individual plants were constrained to grow from seed to the final recorded root system architecture as determined using the μ CT analysis pipeline. The model soil environment was set with homogeneous N distribution as an initial condition, and the plant NUp was simulated over time for each root system scan. A description and guide for using the OpenSimRoot model is provided in Schäfer et al. (2022) and at <https://gitlab.com/rootmodels/OpenSimRoot/-/wikis/home>. For specific details of model parameters and settings used in this study see Data S1.

The model instances for each individual plant were generated using the RSML root system skeleton data output from RooTh. In addition to generating root systems procedurally, OpenSimRoot has the facility to prescribe growth prior to runtime via its input files. This is done by defining the growth direction and rate of each root tip over the desired simulation time, along with the overall branching structure of the root system. A Python script was used to convert the RSML data into the inputs needed by OpenSimRoot. In the absence of intermediate time-point data, growth of each root is assumed to occur at a constant rate from the root's start time to the end of the simulation (generally the age of the plant at the final scan). The growth rate of each root is calculated so that the length of the root measured from the scan matches the length of the model root at the end of the simulation. The start time of each root (other than the primary which starts at time zero) is calculated based on the time the tip of its parent root passes its own start (or origin) point.

For simulations in which intermediate time-series data was used, the OpenSimRoot input was prepared in the same way using the final scan as the model template, except that the intermediate scans were used to adjust the growth rates and start times of each root where necessary. This was done by identifying which roots present in the final scan were present

at each preceding scan and noting its length at that time. Growth rates between successive time-points are then calculated based on this list of lengths over time, again assuming a constant growth rate between data points. Roots that appear in a scan at a given time-point but do not appear at the preceding time-point are assumed to have start times at the preceding time-point or at the time the tip of the parent root passes the roots start point, whichever occurs later. Again, the primary root is given a start time of zero.

Identification or registration of individual roots between scans was done in a semi-automatic way in two stages. First, the primary and seminal roots were matched between scans by rotating about the origin of the primary in the horizontal plane and minimizing differences in the x and y coordinates of the roots (where the z -axis represents depth). Because of the noisy nature of the data, especially around the origin or seed point and at earlier scans, these matches were checked visually by plotting potential matches and correcting errors manually where present. Secondly, after the primary and seminal roots were registered between scans, lateral roots were matched based on branching position and order along the root. Again, these were checked visually, and any identification errors checked manually.

2.5 | Characterization of root system architecture for candidate wheat genotypes contrasting for field NUpE

Four wheat lines from the SXR DH mapping population that contrasted for NUpE, lines 29, 47, 52, and 73, identified in HN and LN field trials, were used in a seedling study with varying soil N nutrition (Table S4). A sandy loam sand mixture (Wissington SPORTS 10 sandy loam [30%]/Wareham bunker sand [70%]; w/w in dry weight basis; 1.3 g cm^{-3} bulk density) (British Sugar plc and D.E. Drew Limited) was prepared. The soil mixture available total N was determined as 17.41 mg kg^{-1} (nitrate 10.84 mg kg^{-1} , ammonium 6.58 mg kg^{-1}) (NRM Laboratories, Bracknell, UK). This nitrate concentration is within the range reported for agricultural soils (Zhu et al., 2021). Forty-eight columns were prepared, half of which were irrigated with modified 3.13 mM NO_3^- 1/4 Hoagland's media and the remaining irrigated with a 0.23 mM NO_3^- 1/4 Hoagland's solution to match the treatments in the time series experiment. Columns were placed in a growth chamber in a randomized block design (four blocks one replicate for each line \times treatment at $20/16^\circ\text{C}$ 16:8 h photoperiod). The soil columns were irrigated from the top every 2 d with either 40 mL HN or LN 1/4 Hoagland's nutrient solution back to field capacity weight. The experiment was staggered over 4 wk with one replicate μCT scanned per week at 9 DAS. Shoots were measured manually using a ruler at destructive harvest.

2.6 | Statistical analysis

Statistical analyses were conducted using R version 4.0.5 (R Development Core Team, 2021); the statistical analysis R codes including the packages needed are available at <https://doi.org/10.5281/zenodo.5504298>. Calculated traits are described in Table S2. Statistical significance of differences between means in the root data was tested with a two-way analysis of variance (ANOVA) using the R package 'lmerTest' (Kuznetsova et al., 2017) and where significant main effects were observed a Tukey's honestly significant difference post hoc test was conducted for multiple pairwise comparisons.

3 | RESULTS

3.1 | Root-soil imaging of wheat seedling using μCT reveals temporal organization of seminal root system and highly plastic lateral roots in response to nitrate

For the time-series seedling study, μCT was used to image root development every 2 d of a high performing NUpE line from the Savannah \times Rialto population (line 47) (Figure 2ab). Plants were grown under a HN and LN treatment with phenotypic variation observed across time and treatment (Figure 2, Table S2). The seminal root system was the dominant root class by length for the first 11 d with the first lateral roots emerging between Day 7 and Day 9 (Figure 2c). By Day 13, the lateral root length was comparable to the seminal root system length (Figure 2c). A significant day \times N treatment interaction was observed for total root length ($p < .001$, Table S2). Under the LN treatment there was a significant increase in seminal root length, seminal root count, and mean lateral root length ($p < .001$, $p < .01$, $p < .05$, respectively, Table S3). At Day 13, there was a significant difference in lateral root length between N treatments with a 73% increase in the LN treatment compared with the HN treatment ($p < .001$, Figure 2c, Table S2). There was also a significant shoot length difference between the N treatments with a 10% greater shoot length in the LN plants at Day 13.

3.2 | NUp simulations using root system architecture extracted from μCT were comparable to a parameterized root growing module using only the final root scan

Using temporal μCT root scans of wheat roots that were scanned every 2 d, the root shapes were imported into the OpenSimRoot model. The root systems for each plant were

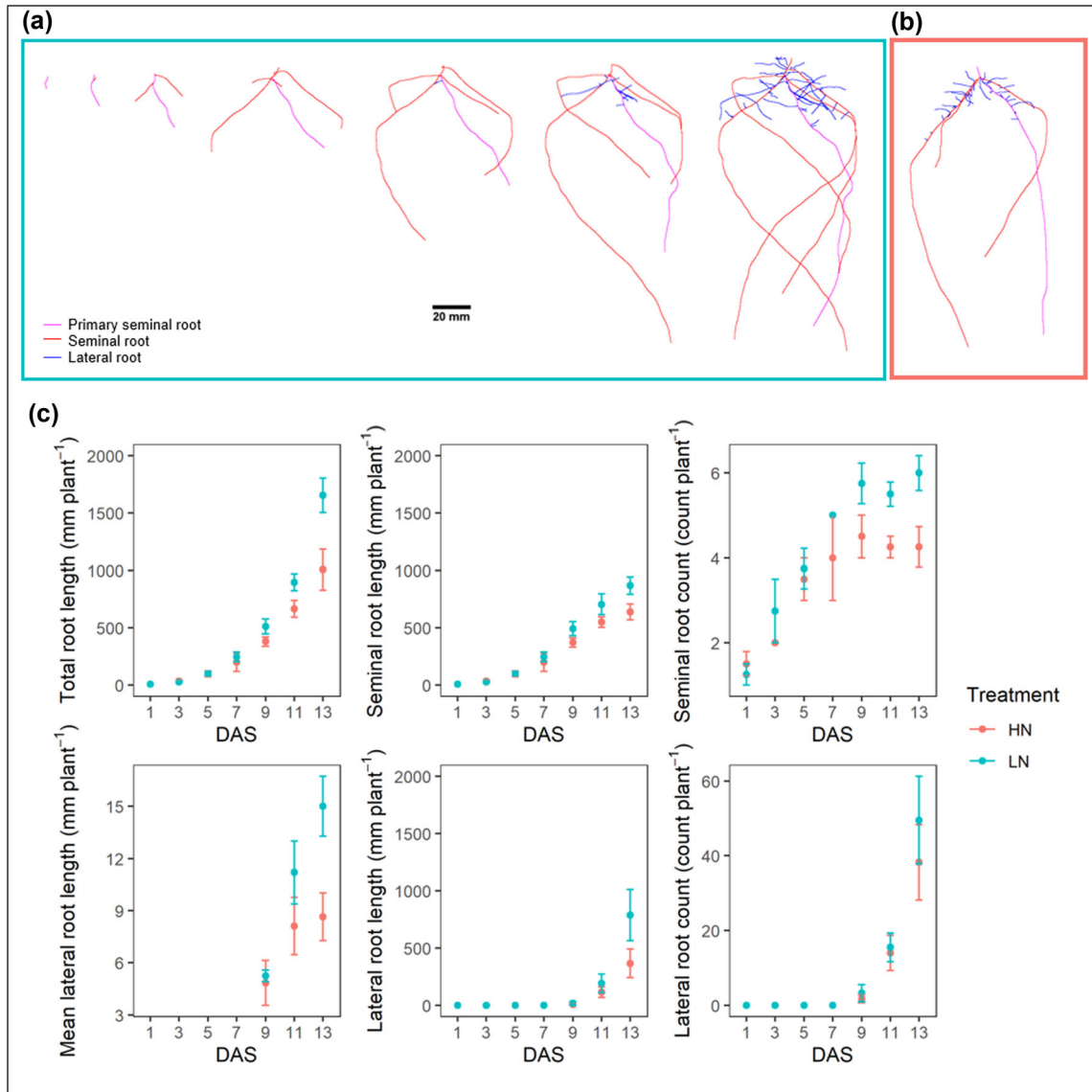


FIGURE 2 Microcomputed tomography (μ CT) time-series analysis reveals the temporal organization of the wheat root system at a resolution of 2 d. The seminal root system of wheat seedlings grown in (a) low and (b) high N showed significant root system differences at 13 d after sowing (DAS). Root classes are color coded as primary seminal (purple), seminal roots (red), and lateral roots (blue). (c): At 13 DAS, a significantly larger root length ($p < .001$) was observed in the low N treatment with an increase in seminal and lateral root length and count traits ($p < .05$)

co-aligned and then simulations were run using the root data with root growth between timepoints. Nitrate uptake by roots was also simulated as the plants grew with a significant day \times N treatment interaction observed for simulated NUp ($p < .001$, Table S3). In the growth and uptake simulations, root system architecture of the LN treated plants had a 35% greater simulated NUp compared with the architecture of HN treated roots at the final timepoint (Figure 3a). Using the time-series μ CT root scans, an exponential NUp curve was observed with the increase in lateral root length in the later time points (Figure 3a). Using only the final μ CT root scan for reference, the NUp simulation closely followed the model using the μ CT time-series scans with a R^2 of 0.93 (Figure 3abc). For NUp rate, a nonlinear increase was observed across time in both

the time-series and final μ CT root simulations with lateral roots having a greater NUp rate than the seminal root system (Figure 3de). Between the time-series and final μ CT root simulations for NUp rate, a positive relationship was observed with an R^2 of 0.55 (Figure 3f).

3.3 | Genetic differences in 3D root system architecture at seedling stage for lines contrasting in field NUpE performance

In the second μ CT study, the root system architecture for Savannah, Rialto, and their four progeny lines from the doubled haploid population with contrasting NUpE were compared. Significant N treatment effects were observed with

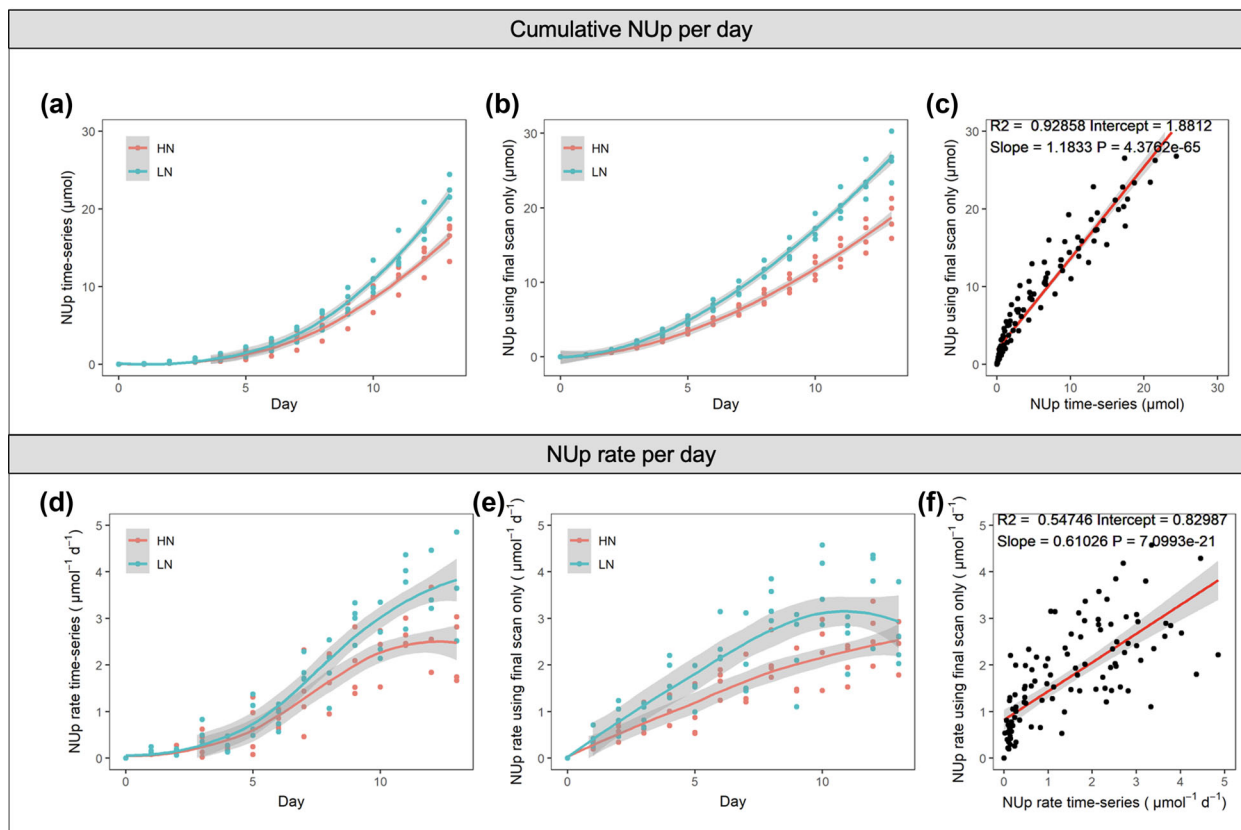


FIGURE 3 OpenSimRoot simulations across time for cumulative NUP per day and NUP rate using time-series root scans and final microcomputed tomography (μ CT) scans only. Cumulative NUP per day simulation using μ CT time-series root scans (a) and final μ CT scans only (b). (c): Cumulative NUP between the two models in A and B was positively correlated ($R^2 = .93$). NUP rate per day simulations across time using μ CT time-series root scans (d) and final μ CT scans only (e). (f): Nitrate uptake rate between the two models in D and E were positively correlated ($R^2 = .55$)

an overall increased lateral root length, increased lateral root count, and shallower seminal root angle, in LN conditions ($p < .05$, Table S4). Significant genotypic differences were observed for lateral root length, lateral root count, lateral root angle, and convex hull traits ($p < .05$, $p < .01$, $p < .05$, $p < .05$, respectively; Table S4). A significant shoot length difference was also observed between wheat lines ($p < .001$; Table S4). Between the high NUpE line 47 and low NUpE line 52, lateral root length and lateral root count were responsible for the root length differences between the lines (Figure 4). Across both N treatments, the high NUpE line had a 74% greater lateral root length and 57% more lateral roots than the low NUpE line (Figure 4c, 4D; $p < .01$).

3.4 | Root traits that affect soil exploration are correlated with NUP and soil-zone depletion of nitrate

As a positive correlation was observed between actual and simulated root growth in the time-series experiment (Figure 3c), simulations were performed on a single-timepoint

experiment containing a larger number of genotypes. A nitrate depletion simulation was also performed using OpenSimRoot. Significant differences in total NUP were found between the high NUpE line 47 and low NUpE line 52 in the simulated study ($p < .05$). This was likely due to the presence of lateral roots later in the time points with a strong correlation between NUP and lateral root length and count (Figure 5a, 5b). A larger root system and therefore convex hull was also positively correlated with NUP (Figure 5c). Values for lateral root and convex hull traits were positively correlated with the size of the nitrate depletion zone in the simulated soil (Figure 5d–5f).

4 | DISCUSSION

Root growth and development directly affects the volume of soil explored for both foraging and interception of water and nutrients. Phenotyping roots without disturbing the root system architecture is a technical challenge with approaches generally destructive or in vitro (Fang et al., 2009; Liu et al., 2021; Tracy et al., 2015; Zeng et al., 2021). Utilizing μ CT for scanning of undisturbed roots in soil provides an unpar-

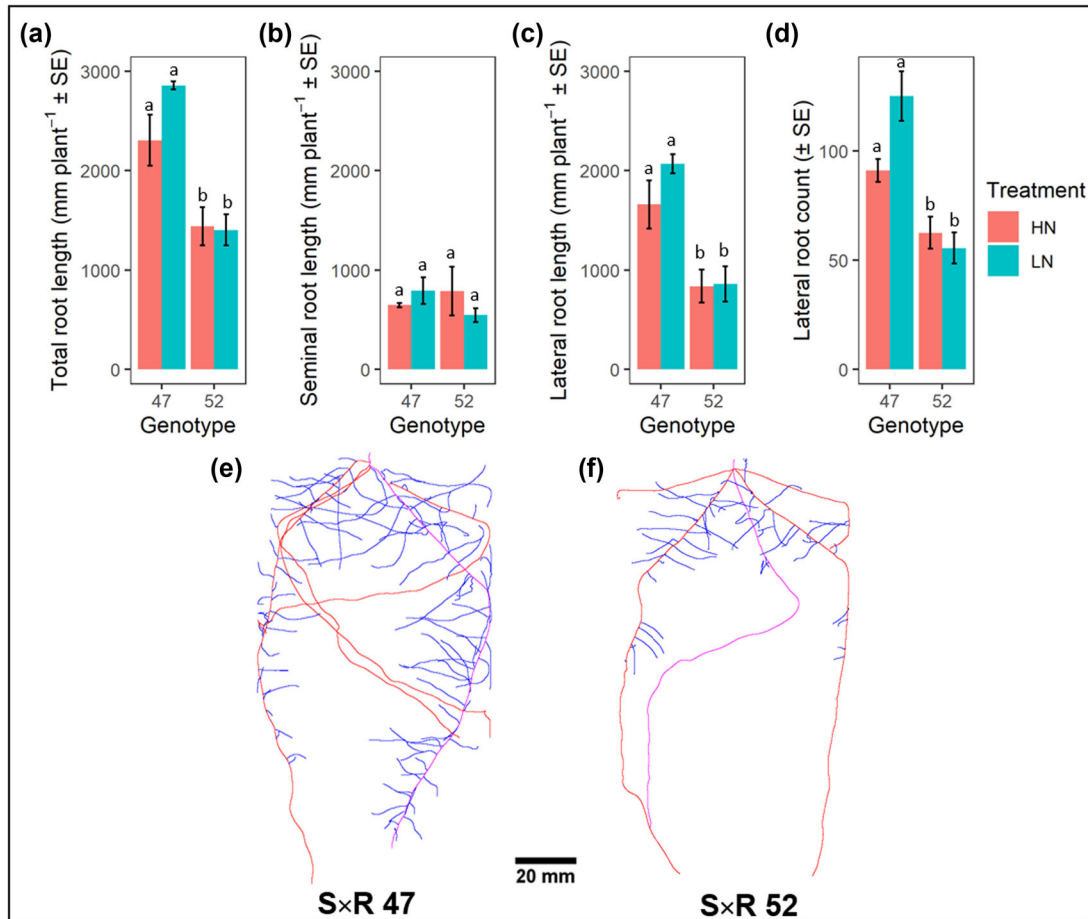


FIGURE 4 Microcomputed tomography (μ CT) analysis reveals the genetic differences in root development of wheat seedlings. Root traits for lines 47 and 52 derived from μ CT scans with significant differences in (a) total root length ($p < .01$), (b) lateral root length ($p < .01$), and (c) lateral root count (LN $p < .01$, HN $p < .05$). Skeletonized root systems for 10-d old wheat seedlings lines (d) 47 and (e) 52. Root classes are color coded as primary seminal (purple), seminal roots (red), and lateral roots (blue). HN, high nitrogen; LN, low nitrogen

alleled opportunity to characterize dynamic rhizosphere processes (Bao et al., 2014; Giri et al., 2018). In the present work, μ CT was used to show that significant N treatment and genotypic differences can be observed in wheat seedling root system architecture at high spatial and temporal resolution.

Roots are plastic in responding to the environment and resource needs. Here we show in soil a significant interaction between plant age and N treatment early in development with increased root length under LN. Nitrate is soluble and therefore mobile and can leach quickly out of the root zone. Lateral roots are particularly responsive to environmental N levels and plant N status (Granato & Raper, 1989; Remans et al., 2006; Weligama et al., 2008; Zhang et al., 1999). A plastic response of greater seminal root length and elongation of lateral roots in LN conditions was observed. These traits can increase soil exploration into new soil zones that would be beneficial for foraging for more resources in low input systems, and the greater root length can help intercept passing nitrate from applied fertilizers in high input systems. Increased length of lateral roots is shown to be advantageous

in N stress (Griffiths et al., 2021; Zhan & Lynch, 2015) with the response observed here a likely beneficial N stress mitigation strategy. Because the seedling root phenotype is significantly influenced by nitrate plasticity how the present phenotype translates in mature plants remains to be determined. Reports of colocalization of quantitative trait loci between seedling root traits and mature crop yield and uptake traits suggest that there is value in appropriate investment strategies in roots (Atkinson et al., 2015; Tuberosa et al., 2002). Scaling root plasticity screens to mapped populations could accelerate discovery in plastic responses and abiotic stress tolerance.

As early root responses to N level were observed in wheat seedlings, soil N content at sowing appears to have important implications on root system architecture. Comparing multiple lines from a doubled haploid mapping population with contrasting field NUpE measured at physiological maturity, significant genotypic differences were observed for lateral root length, lateral count, lateral angle, and convex hull representing the potential variation to exploit for improving rooting traits and N uptake. Among the candidate wheat lines

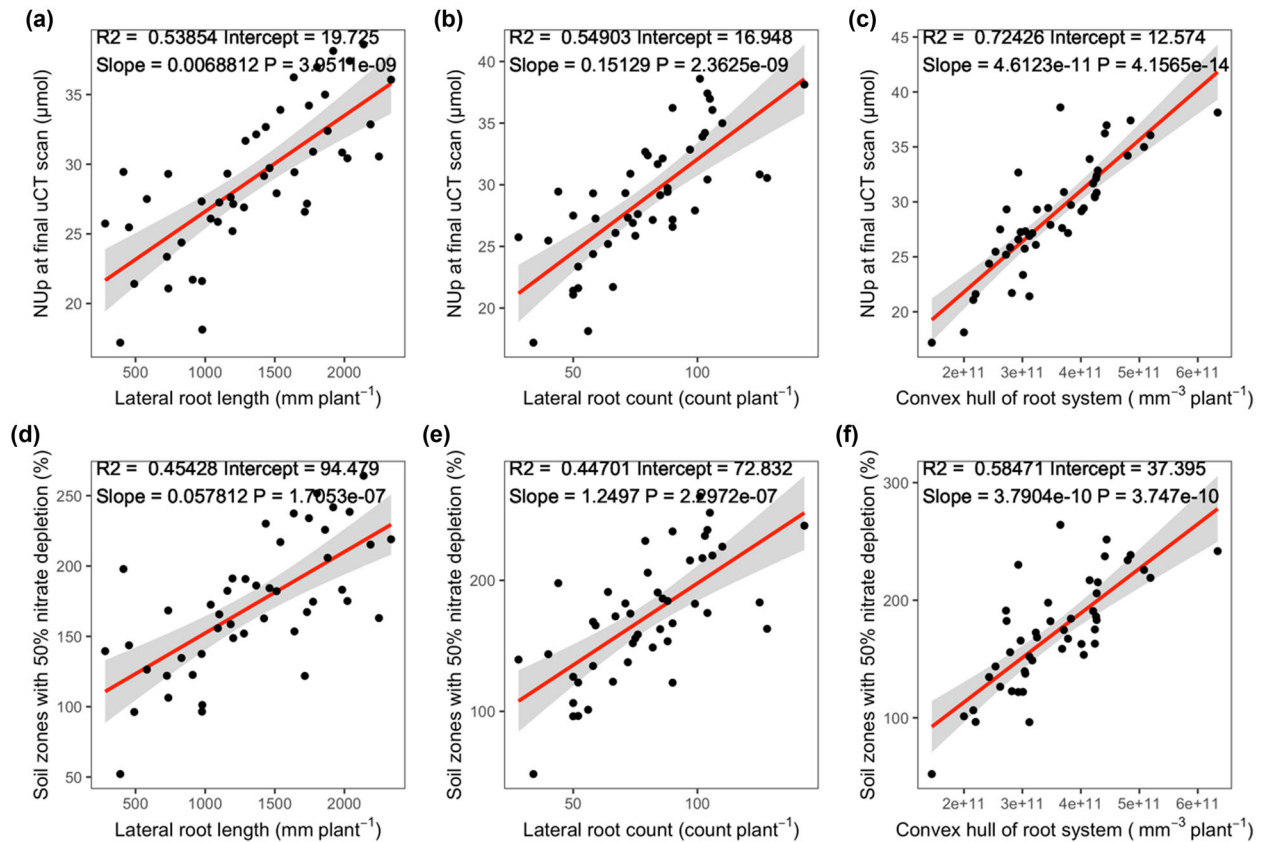


FIGURE 5 Correlation analyses for microcomputed tomography (μ CT) root system architecture traits with nitrate uptake among the selected Savannah \times Rialto winter wheat doubled (SXR DH) lines and parents using OpenSimRoot. Positive correlation between NUp at end of simulation and (a) lateral root length, (b) lateral root count, and (c) convex hull of root system. Positive correlation between percentage of soil with 50% nitrate depletion at end of simulation and (d) lateral root length, (e) lateral root count, and (f) convex hull of root system

tested, the high NUpE line 47 had a significantly greater lateral root length and lateral root count than the low NUpE line 52. Greater lateral root length at this early stage may be a beneficial investment trait as it will allow greater soil exploration for nitrate earlier in the season and may provide a cumulative benefit of N uptake. Selecting wheat lines based on early vigor lateral root traits, therefore, may be beneficial for selecting greater field performance lines (Wang et al., 2018). Moreover, the seminal roots penetrate to a depth of more than 1.5 m in field soils, become the deepest roots (Araki & Iijima, 2001) and are the most important for capture of N from the deep soil layers during grain filling under N limitation. The diversity observed in root plasticity to nitrate within the tested doubled haploid population subset lines poses the potential to find the underlying genetics involved for root plasticity to nitrate.

The holistic plant model OpenSimRoot was used to simulate NUp by the plants in a simulated soil environment using the μ CT root system architecture (Postma et al., 2017). Two-day temporal resolution μ CT scans were co-aligned and then used as reference points in a nonlinear root growth model. Across the root growth simulation, NUp was also simulated by roots using the extracted root system architecture. The param-

eterized model was then used to compare against a simulation using only the final μ CT root system as a reference. A strong positive correlation between the two model types was observed for NUp that validates scaling up this approach without the need of high-temporal root shape information once the model is parameterized and implying root growth rate is generally linear. Greater variation was observed in the simulated NUp rate between the two model types than the cumulative NUp, which likely represents inaccuracy in the emergence and growth of lateral roots that drive the majority of the uptake in the simulations. Further study into defining the differential growth rates of roots by age and root type would be useful for further model parameterization.

Continued exploration of roots into new soil domains may provide more resources to forage. As expected, root length positively correlated with NUp in the simulations with lateral root length and lateral root count being key drivers in root distribution for uptake. The simulations ran in this study used real root system architectures as extracted from μ CT scans and were simulated without plant neighbors. Intra-root competition for nitrate is an important property to consider for optimal root system architecture; depending on the soil type,

plant density, N fixation, and fertilizer management strategy, the soil will exhibit localized depletion by root uptake. In the field, lateral soil exploration poses greater inter-plant competition than vertical exploration, which would be important to consider in future simulations. The cost of having an extensive root system would also be important to consider in longer simulations where the nitrate environment can become depleted or when more N can enter the system. Intra- and inter-root competition is not an efficient use of resources as the increased metabolic cost outweighs the benefit of a relatively small gain in resource capture (Lynch & Ho, 2005; Nielsen et al., 1994; van Vuuren et al., 1996).

Using temporal μ CT imaging and simulation, we demonstrated genotypic and N treatment variation in root system architecture. Comparing wheat lines exhibiting differential NUpE in field trials, we show that greater lateral root length, lateral root count, and convex hull size during seedling establishment may be a predictive trait for increased NUpE. By conducting temporal root analysis and simulation, we demonstrate that a root growth and NUp model with a 2-d temporal resolution reference was comparable to a model that only utilized the final root system shape. Utilizing nondestructive root phenotyping approaches and simulation fusion will be important aspects of functional phenomics (York, 2019) of rhizosphere processes and root system architecture traits for breeding of more resource efficient crops.

DATA AVAILABILITY STATEMENT

The dataset and R code supporting the results of this article are available at: <https://doi.org/10.5281/zenodo.5504298>.

ACKNOWLEDGMENTS

This work was supported by the European Research Council FUTUREROOTS Advanced Investigator grant [grant number 294729] and by the Biotechnology and Biological Sciences Research Council [grant numbers BB/L026848/1 and BB/P026834/1]. SM, CS, MJB and TPP are also supported by the Biotechnology and Biological Sciences Research Council Designing Future Wheat Cross-Institute Strategic Programme [grant no. BB/P016855/1].

AUTHOR CONTRIBUTIONS

Marcus Griffiths: Conceptualization; Formal analysis; Investigation; Writing – original draft; Writing – review & editing. Nathan Mellor: Formal analysis; Writing – original draft; Writing – review & editing. Craig J. Sturrock: Investigation; Methodology; Supervision; Writing – review & editing. Brian S. Atkinson: Investigation; Writing – review & editing. James Johnson: Software; Writing – review & editing. Stefan Mairhofer: Software; Writing – review & editing. Larry M. York: Formal analysis; Writing – review & editing. Jonathan A. Atkinson: Project administration; Supervision; Writing – review & editing. Mohammadreza Soltaninejad: Software; Writing – review & editing. John F. Foulkes: Resources; Supervision; Writing – review & editing. Michael P. Pound: Software; Supervision; Writing – review & editing. Sacha J. Mooney: Project administration; Supervision; Writing – review & editing. Tony P. Pridmore: Project administration; Software; Supervision; Writing – review & editing. Malcolm J. Bennett: Conceptualization; Funding acquisition; Project administration; Supervision; Writing – review & editing. Darren M. Wells: Conceptualization; Project administration; Supervision; Writing – original draft; Writing – review & editing.

jad: Software; Writing – review & editing. John F. Foulkes: Resources; Supervision; Writing – review & editing. Michael P. Pound: Software; Supervision; Writing – review & editing. Sacha J. Mooney: Project administration; Supervision; Writing – review & editing. Tony P. Pridmore: Project administration; Software; Supervision; Writing – review & editing. Malcolm J. Bennett: Conceptualization; Funding acquisition; Project administration; Supervision; Writing – review & editing. Darren M. Wells: Conceptualization; Project administration; Supervision; Writing – original draft; Writing – review & editing.

CONFLICT OF INTEREST

The authors declare that the research was conducted in the absence of any commercial or financial relationships that could be construed as a potential conflict of interest.

ORCID

Marcus Griffiths  <https://orcid.org/0000-0003-2349-8967>

Nathan Mellor  <https://orcid.org/0000-0002-0498-0996>

Craig J. Sturrock  <https://orcid.org/0000-0002-5333-8502>

Brian S. Atkinson  <https://orcid.org/0000-0001-8791-1613>

Larry M. York  <https://orcid.org/0000-0002-1995-9479>

Jonathan A. Atkinson  <https://orcid.org/0000-0003-2815-0812>

Mohammadreza Soltaninejad  <https://orcid.org/0000-0002-9889-4369>

John F. Foulkes  <https://orcid.org/0000-0002-7765-8340>

Michael P. Pound  <https://orcid.org/0000-0002-5016-1078>

Sacha J. Mooney  <https://orcid.org/0000-0002-9314-8113>

Tony P. Pridmore  <https://orcid.org/0000-0002-9485-1978>

Malcolm J. Bennett  <https://orcid.org/0000-0003-0475-390X>

Darren M. Wells  <https://orcid.org/0000-0002-4246-4909>

REFERENCES

- Araki, H., & Iijima, M. (2001). Deep rooting in winter wheat: Rooting nodes of deep roots in two cultivars with deep and shallow root systems. *Plant Production Science*, 4(3), 215–219. <https://doi.org/10.1626/pps.4.215>
- Miller A. J., Fan X., Orsel M., Smith S. J., & Wells D. M. (2007). Nitrate transport and signalling. *Journal of Experimental Botany*, 58(9), 2297–2306. <https://doi.org/10.1093/jxb/erm066>
- Arsenault, J.-L., Poulcur, S., Messier, C., & Guay, R. (1995). WinRHIZO™, a root-measuring system with a unique overlap correction method. *Hortscience*, 30(4). <https://doi.org/10.21273/hortsci.30.4.906d>
- Atkinson, J. A., Wingen, L. U., Griffiths, M., Pound, M. P., Gaju, O., Foulkes, M. J., le Gouis, J., Griffiths, S., Bennett, M. J., King, J., & Wells, D. M. (2015). Phenotyping pipeline reveals major seedling root growth QTL in hexaploid wheat. *Journal of Experimental Botany*, 66(8), 2283–2292. <https://doi.org/10.1093/jxb/erv006>
- Atkinson, J. A., Hawkesford, M. J., Whalley, W. R., Zhou, H., & Mooney, S. J. (2020). Soil strength influences wheat root interactions with soil

- macropores. *Plant Cell and Environment*, 43(1), 235–245. <https://doi.org/10.1111/pce.13659>
- Bao, Y., Aggarwal, P., Robbins, N. E., Sturrock, C. J., Thompson, M. C., Tan, H. Q., Tham, C., Duan, L., Rodriguez, P. L., Vernoux, T., Mooney, S. J., Bennett, M. J., & Dinnyen, J. R. (2014). Plant roots use a patterning mechanism to position lateral root branches toward available water. *Proceedings of the National Academy of Sciences of the United States of America*, 111(25), 9319–9324. <https://doi.org/10.1073/pnas.1400966111>
- Fang, S., Yan, X., & Liao, H. (2009). 3D reconstruction and dynamic modeling of root architecture in situ and its application to crop phosphorus research. *Plant Journal*, 60(6), 1096–1108. <https://doi.org/10.1111/j.1365-3113X.2009.04009.x>
- Foulkes, M. J., Hawkesford, M. J., Barraclough, P. B., Holdsworth, M. J., Kerr, S., Kightley, S., & Shewry, P. R. (2009). Identifying traits to improve the nitrogen economy of wheat: Recent advances and future prospects. *Field Crops Research*, 114, 329–342. <https://doi.org/10.1016/j.fcr.2009.09.005>
- Giri, J., Bhosale, R., Huang, G., Pandey, B. K., Parker, H., Zappala, S., Yang, J., Dievart, A., Bureau, C., Ljung, K., Price, A., Rose, T., Larriou, A., Mairhofer, S., Sturrock, C. J., White, P., Dupuy, L., Hawkesford, M., Perin, C., ..., Bennett, M. J. (2018). Rice auxin influx carrier OsAUX1 facilitates root hair elongation in response to low external phosphate. *Nature Communications*, 9. <https://doi.org/10.1038/s41467-018-03850-4>
- Granato, T. C., & Raper, C. D. (1989). Proliferation of maize (*Zea mays* L.) roots in response to localized supply of nitrate. *Journal of Experimental Botany*, 40(2), 263–275. <https://doi.org/10.1093/jxb/40.2.263>
- Guo, H., Ayalew, H., Seethepalli, A., Dhakal, K., Griffiths, M., Ma, X. F., & York, L. M. (2021). Functional phenomics and genetics of the root economics space in winter wheat using high-throughput phenotyping of respiration and architecture. *New Phytologist*, 232(1), 98–112. <https://doi.org/10.1111/nph.17329>
- Griffiths, M., Wang, X., Dhakal, K., Guo, H., Seethepalli, A., Kang, Y., & York, L. M. (2021). Interactions among rooting traits for deep water and nitrogen uptake in upland and lowland ecotypes of switchgrass (*Panicum virgatum* L.). *Journal of Experimental Botany*, 73(3), 967–969. <https://doi.org/10.1093/jxb/erab437>
- Griffiths, M., & York, L. M. (2020). Targeting root ion uptake kinetics to increase plant productivity and nutrient use efficiency. *Plant Physiology*, 182(4), 1854–1868. <https://doi.org/10.1104/pp.19.01496>
- Ho, M. D., Rosas, J. C., Brown, K. M., & Lynch, J. P. (2005). Root architectural tradeoffs for water and phosphorus acquisition. *Functional Plant Biology*, 32(8), 737–748. <https://doi.org/10.1071/FP05043>
- Kuznetsova, A., Brockhoff, P. B., & Christensen, R. H. B. (2017). lmerTest Package: Tests in Linear Mixed Effects Models. *Journal of Statistical Software*, 82(13), 1–26. <https://doi.org/10.18637/jss.v082.i13>
- Lark, R. M., Milne, A. E., Addiscott, T. M., Goulding, K. W. T., Webster, C. P., & O'Flaherty, S. (2004). Scale- and location-dependent correlation of nitrous oxide emissions with soil properties: An analysis using wavelets. *European Journal of Soil Science*, 55, 611–627. <https://doi.org/10.1111/j.1365-2389.2004.00620.x>
- Liu, S., Barrow, C. S., Hanlon, M., Lynch, J. P., & Bucksch, A. (2021). DIRT/3D: 3D root phenotyping for field-grown maize (*Zea mays*). *Plant Physiology*, 187(2), 737–757. <https://doi.org/10.1093/plphys/kiab311>
- Lobet, G., Pound, M. P., Diener, J., Pradal, C., Draye, X., Godin, C., Javaux, M., Leitner, D., Meunier, F., Nacry, P., Pridmore, T. P., & Schnepf, A. (2015). Root system markup language: Toward a unified root architecture description language. *Plant Physiology*, 167(3), 617–627. <https://doi.org/10.1104/pp.114.253625>
- Lynch, J. P. (2013). Steep, cheap and deep: An ideotype to optimize water and N acquisition by maize root systems. *Annals of Botany*, 112(2), 347–357. <https://doi.org/10.1093/aob/mcs293>
- Lynch, J. P., & Ho, M. D. (2005). Rhizoeconomics: Carbon costs of phosphorus acquisition. *Plant and Soil*, 269, 45–56. <https://doi.org/10.1007/s11104-004-1096-4>
- Manske, G. G. B., Ortiz-Monasterio, J. I., & Vlek, P. L. D. (2001). Techniques for measuring genetic diversity in roots. In M. P. Reynolds, J. I. Ortiz-Monasterio, & A. McNab (Eds.), *Application of physiology in wheat breeding* (pp. 208–218). CIMMYT.
- Mairhofer, S., Sturrock, C., Wells, D. M., Bennett, M. J., Mooney, S. J., & Pridmore, T. P. (2014). On the evaluation of methods for the recovery of plant root systems from X-ray computed tomography images. *Functional Plant Biology*, 42(5), 460–470. <https://doi.org/10.1071/FP14071>
- Mairhofer, S., Pridmore, T., Johnson, J., Wells, D. M., Bennett, M. J., Mooney, S. J., & Sturrock, C. J. (2018). X-ray computed tomography of crop plant root systems grown in soil. *Current Protocols in Plant Biology*. <https://doi.org/10.1002/cppb.20049>
- Mooney, S. J. (2002). Three-dimensional visualization and quantification of soil macroporosity and water flow patterns using computed tomography. *Soil Use and Management*, 18(2), 142–151. <https://doi.org/10.1111/j.1475-2743.2002.tb00232.x>
- Morris, E. C., Griffiths, M., Golebiowska, A., Mairhofer, S., Burr-Hersey, J., Goh, T., von Wangenheim, D., Atkinson, B., Sturrock, C. J., Lynch, J. P., Vissenberg, K., Ritz, K., Wells, D. M., Mooney, S. J., & Bennett, M. J. (2017). Shaping 3D root system architecture. *Current Biology*, 27(17), PR919–R930. <https://doi.org/10.1016/j.cub.2017.06.043>
- Nagel, K. A., Lenz, H., Kastenholz, B., Gilmer, F., Aversch, A., Putz, A., Heinz, K., Fischbach, A., Scharr, H., Fiorani, F., Walter, A., & Schurr, U. (2020). The platform GrowScreen-Agar enables identification of phenotypic diversity in root and shoot growth traits of agar grown plants. *Plant Methods*, 16(1), 1–17. <https://doi.org/10.1186/s13007-020-00631-3>
- Nielsen, K. L., Lynch, J. P., Jablókow, A. G., & Curtis, P. S. (1994). Carbon cost of root systems: An architectural approach. *Plant and Soil*, 165(1), 161–169. <https://doi.org/10.1007/BF00009972>
- Postma, J. A., Kuppe, C., Owen, M. R., Mellor, N., Griffiths, M., Bennett, M. J., Lynch, J. P., & Watt, M. (2017). OpenSimRoot: Widening the scope and application of root architectural models. *New Phytologist*, 215(3), 1274–1286. <https://doi.org/10.1111/nph.14641>
- R Core Team. (2021). *R: A language and environment for statistical computing*. R Foundation for Statistical Computing. <https://www.R-project.org/>
- Remans, T., Nacry, P., Pervent, M., Filleul, S., Diatloff, E., Mounier, E., Tillard, P., Forde, B. G., & Gojon, A. (2006). The Arabidopsis NRT1.1 transporter participates in the signaling pathway triggering root colonization of nitrate-rich patches. *Proceedings of the National Academy of Sciences of the United States of America*, 103(50), 19206–19211. <https://doi.org/10.1073/pnas.0605275103>
- Rogers, E. D., & Benfey, P. N. (2015). Regulation of plant root system architecture: Implications for crop advancement. *Current Opinion in Biotechnology*, 32, 93–98. <https://doi.org/10.1016/j.copbio.2014.11.015>

- Rowell, D. L. (1994). *Soil science: Methods & applications*. Routledge. <https://doi.org/10.4324/9781315844855>
- Schäfer, E. D., Owen, M. R., Postma, J. A., Kuppe, C., Black, C. K., & Lynch, J. P. (2022). Simulating crop root systems using OpenSim-Root. In M. Lucas (Ed.), *Plant systems biology: Methods in molecular biology* (Vol. 2395, pp. 293–323). Springer. https://doi.org/10.1007/978-1-0716-1816-5_15
- Smucker, A. J. M., Mcburney, S. L., & Srivastava, A. K. (1982). Quantitative separation of roots from compacted soil profiles by the hydro-pneumatic elutriation system. *Agronomy*, 72, 500–503. <https://doi.org/10.2134/agronj1982.00021962007400030023x>
- Soltaninejad, M., Sturrock, C. J., Griffiths, M., Pridmore, T. P., & Pound, M. P. (2020). Three dimensional root CT segmentation using multi-resolution encoder-decoder networks. *IEEE Transactions on Image Processing*, 29, 6667–6679. <https://doi.org/10.1109/TIP.2020.2992893>
- Topp, C. N., Iyer-Pascuzzi, A. S., Anderson, J. T., Lee, C. R., Zurek, P. R., Symonova, O., Zheng, Y., Bucksch, A., Milekyo, Y., Galkovskyi, T., Moore, B. T., Harer, J., Edelsbrunner, H., Mitchell-Olds, T., Weitz, J. S., & Benfey, P. N. (2013). 3D phenotyping and quantitative trait locus mapping identify core regions of the rice genome controlling root architecture. *Proceedings of the National Academy of Sciences of the United States of America*, 110(18), E1695–E1704. <https://doi.org/10.1073/pnas.1304354110>
- Tracy, S. R., Mooney, S. J., Sturrock, C. J., Mairhofer, S., Al-Traboulsi, M., Bennett, M. J., Pridmore, T. P., Lynch, J. P., & Wells, D. M. (2015). Laboratory and field techniques for measuring root distribution and architecture. In C. K. Ong, C. R. Black, & J. Wilson (Eds) *Tree-crop interactions: Agroforestry in a changing climate* (2nd ed., pp. 258–277). C.A.B International.
- Tuberosa, R., Salvi, S., Sanguineti, M. C., Landi, P., Maccaferri, M., & Conti, S. (2002). Mapping QTLs regulating morpho-physiological traits and yield: Case studies, shortcomings and perspectives in drought-stressed maize. *Annals of Botany*, 89, 941–963. <https://doi.org/10.1093/aob/mcf134>
- van Dusschoten, D., Metzner, R., Kochs, J., Postma, J. A., Pflugfelder, D., Bühler, J., Schurr, U., & Jahnke, S. (2016). Quantitative 3D analysis of plant roots growing in soil using magnetic resonance imaging. *Plant Physiology*, 170(3), 1176–1188. <https://doi.org/10.1104/pp.15.01388>
- van Vuuren, M. M., Robinson, D., & Griffiths, B. S. (1996). Nutrient inflow and root proliferation during the exploitation of a temporally and spatially discrete source of nitrogen in soil. *Plant and Soil*, 178, 185–192. <https://doi.org/10.1007/BF00011582>
- Wang, F., Longkumer, T., Catausan, S. C., Calumpang, C. L. F., Tarun, J. A., Cattin-Ortola, J., Ishizaki, T., Pariasca Tanaka, J., Rose, T., Wissuwa, M., & Kretschmar, T. (2018). Genome-wide association and gene validation studies for early root vigour to improve direct seeding of rice. *Plant Cell and Environment*, 41(12), 2731–2743. <https://doi.org/10.1111/pce.13400>
- Weligama, C., Tang, C., Sale, P. W. G., Conyers, M. K., & Liu, D. L. (2008). Localised nitrate and phosphate application enhances root proliferation by wheat and maximises rhizosphere alkalisation in acid subsoil. *Plant and Soil*, 312, 101–115. <https://doi.org/10.1007/s11104-008-9581-9>
- York, L. M. (2019). Functional phenomics: An emerging field integrating high-throughput phenotyping, physiology, and bioinformatics. *Journal of Experimental Botany*, 70(2), 379–386. <https://doi.org/10.1093/jxb/ery379>
- Zeng, D., Li, M., Jiang, N., Ju, Y., Schreiber, H., Chambers, E., Letscher, D., Ju, T., & Topp, C. N. (2021). TopoRoot: A method for computing hierarchy and fine-grained traits of maize roots from 3D imaging. *Plant Methods*, 17(1), 127. <https://doi.org/10.1186/s13007-021-00829-z>
- Zhan, A., & Lynch, J. P. (2015). Reduced frequency of lateral root branching improves N capture from low-N soils in maize. *Journal of Experimental Botany*, 66(7), 2055–2065. <https://doi.org/10.1093/jxb/erv007>
- Zhang, H., Jennings, A., Barlow, P. W., & Forde, B. G. (1999). Dual pathways for regulation of root branching by nitrate. *Proceedings of the National Academy of Sciences of the United States of America*, 96(11), 6529–6534. <https://doi.org/10.1073/pnas.96.11.6529>
- Zhou, H., Whalley, W. R., Hawkesford, M. J., Ashton, R. W., Atkinson, B., Atkinson, J. A., Sturrock, C. J., Bennett, M. J., & Mooney, S. J. (2021). The interaction between wheat roots and soil pores in structured field soil. *Journal of Experimental Botany*, 72(2), 747–756. <https://doi.org/10.1093/jxb/eraa475>
- Zhu, Y., Chen, Y., Ali, M. A., Dong, L., Wang, X., Archontoulis, S. v., Schnable, J. C., & Castellano, M. J. (2021). Continuous in situ soil nitrate sensors: The importance of high-resolution measurements across time and a comparison with salt extraction-based methods. *Soil Science Society of America Journal*, 85(3), 677–690. <https://doi.org/10.1002/saj2.20226>

SUPPORTING INFORMATION

Additional supporting information may be found in the online version of the article at the publisher's website.

How to cite this article: Griffiths, M., Mellor, N., Sturrock, C. J., Atkinson, B. S., Johnson, J., Mairhofer, S., York, L. M., Atkinson, J. A., Soltaninejad, M., Foulkes, J. F., Pound, M. P., Mooney, S. J., Pridmore, T. P., Bennett, M. J., & Wells, D. M. (2022). X-ray CT reveals 4D root system development and lateral root responses to nitrate in soil. *Plant Phenome Journal*, 5, e20036. <https://doi.org/10.1002/ppj2.20036>